Polarization Sensing with Visual Detection

ARTICLE *in* ANALYTICAL CHEMISTRY · MAY 1999

Impact Factor: 5.64 · DOI: 10.1021/ac981301i · Source: PubMed

3 AUTHORS, INCLUDING:

Joseph R Lakowicz
University of Maryland Medical Center
878 PUBLICATIONS **42,262** CITATIONS

Anal. Chem. **1999,** *71,* 1241−1251

Accelerated Articles

Polarization Sensing with Visual Detection

Ignacy Gryczynski, Zygmunt Gryczynski, and Joseph R. Lakowicz*

Center for Fluorescence Spectroscopy, Department of Biochemistry and Molecular Biology, University of Maryland School of Medicine, 725 West Lombard Street, Baltimore, Maryland 21201

We describe a new approach to fluorescence sensing which relies on visual determination the polarization. The sensing device consists of a fluorescent probe, which changes intensity in responses to the analyte, and an oriented fluorescent film, which is not affected by the analyte. An emission filter is selected to observe the emission from both the film and the sensing fluorophore. Changes in the probe intensity result in changes in the polarization of the combined emission from the sensor and reference. The degree of polarization can be detected visually using a dual polarizer with adjacent sections oriented orthogonally to each other. The emission passing through the dual polarizer is viewed with a second analyzing polarizer. This analyzer is rotated manually to yield equal intensities from both sides of the dual polarizer. This approach was used to measure the concentration of RhB in intralipid and to measure pH using 6-carboxyfluorescein. The analyzer angle is typically accurate to 1°, providing pH values accurate to ±0.1 pH unit at the midpoint of the titration curve. We also describe a method of visual polarization sensing that does not require an oriented film and that can use the same fluorophore for the sample and reference. These approaches to visual sensing are generic and can be applied to a wide variety of analytes for which fluorescent probes are available. Importantly, the devices are simple, with the only electronic component being the light source.

During the past 10 years there have been remarkable advances in the technology for fluorescence sensing.[1−7] There has been extensive development of new fluorescent probes[8−10] and the introduction of time-resolved fluorescence to chemical sensing, which is referred to as lifetime-based sensing.[11−13] Additionally, the time scale of fluorescence has been extended from the nanosecond range to the microsecond range by the use of long-lifetime metal−ligand complexes.[14,15]

New approaches to fluorescence sensing continue to appear. During the past year, a new approach to sensing was developed which uses reference fluorophores in addition to the sensing fluorophores. The concept is to mix a sensing fluorophore that is sensitive to analyte with a second fluorophore that is not sensitive to analyte. One then measures the combined emission of the sensor and reference fluorophores, which can be used to determine the analyte concentration. This approach has been used with the long-lifetime metal−ligand complexes (MLC) as the reference

(1) Spichiger-Keller, U. E. *Chemical Sensors and Biosensors for Medical and Biological Applications*; Wiley-VCH: New York, 1998; p 413.
(2) Kunz, R. E., Ed. *Sens. Actuators B* **1997**, *B38*, 1−188; **1997**, *B39*, 1−468 (Proc. of 3rd European Conference on Optical Chemical Sensors and Biosensors, Europt(R)odeIII).
(3) Thompson, R. B., Ed. *SPIE Proc.* **1997**, *2980*, 582.
(4) Lakowicz, J. R., Ed. *Topics in Fluorescence Spectroscopy, Volume 4: Probe Design and Chemical Sensing*; Plenum Press: New York, 1994; p 501.
(5) Schulman, S. G., Ed. *Molecular Luminescence Spectroscopy, Methods and Applications: Part 3*; John Wiley & Sons: New York, 1993; p 467.
(6) Wolfbeis, O. S., Ed. *Fiber Optic Chemical Sensors and Biosensors*; CRC Press: Boca Raton, 1991; Vol. 1, p 413.
(7) Wolfbeis, O. S., Ed. *Fiber Optic Chemical Sensors and Biosensors*; CRC Press: Boca Raton, 1991; Vol. 2, p 358.
(8) Haugland, R. P. *Handbook of Fluorescent Probes and Research Chemicals*; Spence, T. Z., Ed.; Molecular Probes, Inc.: Eugene, OR, 1996; p 679.
(9) Slavik, J., Ed. *Fluorescence Microscopy and Fluorescent Probes*; Plenum Press: New York, 1998; Vol. 2, p 272.
(10) Czarnik, A. W., Ed. *Fluorescent Chemosensors for Ion and Molecule Recognition*; ACS Symposium Series 538; American Chemical Society: Washington, DC, 1993; p 235.
(11) Lippitsch, M. E.; Draxler, S.; Kieslinger, D. *Sens. Actuators B* **1997**, *38*−*39*. 96−102.
(12) Lippitsch, M. E.; Pusterhofer, J.; Leiner, M. J. P.; Wolfbeis, O. S. *Anal. Chim. Acta* **1998**, *205*, 1−6.
(13) Szmacinski, H.; Lakowicz, J. R. Lifetime-based sensing. In *Topics in Fluorescence Spectroscopy: Vol. 4: Probe Design and Chemical Sensing*; Lakowicz, J. R., Ed.; Plenum Press: New York, 1994; pp 295−334.
(14) Terpetschnig, E.; Szmacinski, H.; Lakowicz, J. R. Long-lifetime metal−ligand complexes as probes in biophysics and clinical chemistry. In *Methods in Enzymology*; Academic Press: New York, 1997; Vol. 278, pp 295−321.
(15) Szmacinski, H.; Castellano, F. N.; Terpetschnig, E.; Dattelbaum, J. D.; Lakowicz, J. R.; Meyer, G. J. *Biochim. Biophys. Acta* **1997**, *1383*, 151−159.

10.1021/ac981301i CCC: $18.00
Published on Web 02/18/1999

fluorophore and a pH-sensitive probe, to determine pH or pCO_2 from the phase angle of the emission.[16,17] In this laboratory, we have also used such mixtures to determine pH, calcium, and glucose concentrations. In our studies, we used the low-frequency modulation of the emission, rather than the phase angle, to determine the analyte concentration.[18−21] We showed that the low-frequency modulation can be used to determine the fractional intensity of the nanosecond fluorophore, relative to that of the metal−ligand complex with its microsecond decay time.

In a recently submitted paper,[22] we extended the idea of using a reference fluorophore to sensing based on anisotropy measurements. The concept is based on the additivity of anisotropy.[23−25] This rule states that the anisotropy for a mixture of fluorophores is the weighted average of the value for each fluorophore and their fractional contributions to the total intensity. We developed sensing methods in which the reference was a fluorophore in a stretch-oriented film of poly(vinyl alcohol). We used anisotropy-based sensing to measure pH using 6-carboxyfluorescein or the concentration of labeled protein in the sample.[22]

While the sensing methods described above can be accomplished with simple devices, it is desirable to further simplify the measurements. Hence we developed a method to perform anisotropy-based sensing with visual detection. This work was stimulated by the concepts shown in Chart 1. We imagined that back-illuminated hand-held devices could be used for point-of-care medical testing (top). Alternatively, it would be valuable to have watchlike devices that can perform measurements through the skin (bottom). The basic idea is for the doctor or patient to perform the measurement by visual comparison of two intensities. These fluorescent intensities will be seen side by side through a pair of adjacent crossed polarizers, as shown on the face of the watch (Chart 1, lower panel). The analyte concentration will determine the relative intensities seen through each polarizer orientation. The polarization or anisotropy of the sample can be determined by simple rotation of the analyzer polarizer to yield equal intensities for each side of the crossed polarizer. With such a device, the only required electronics is for the light source. Hence, one can readily imagine portable battery-powered devices for measurement of blood gases, electrolytes, glucose, and a wide variety of analytes.

Chart 1. Anisotropy-Based Sensing for Blood Chemistry and Transdermal Measurements[a]

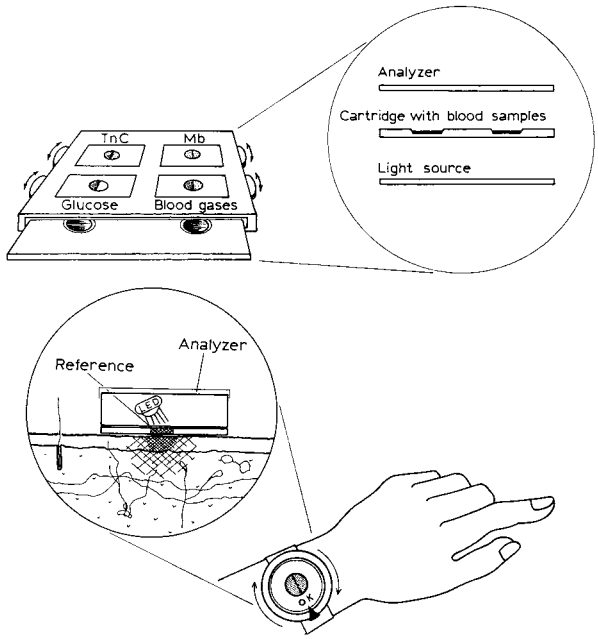

[a] (top) The excitation source, sample, and detector in an in-line geometry. (bottom) The fluorescence from the implanted patch and/or tissue is observed using front-face geometry.

MATERIALS AND METHODS

N-Methyl-4-(pyrrolidinyl)styrylpyridinium iodide (MPSPI) was obtained from Molecular Probes (Eugene, OR), rhodamine B (RhB) was from Exciton, Inc. (Dayton, OH), and 6-carboxyfluorescein (6-CF) was from Eastman Kodak (Rochester, NY). Intralipid (20%) was obtained from Kabi Vitrum, Inc. (Clayton, NC) and diluted 40-fold to 0.5%, in 50 mM tris buffer at the desired pH values.

Several excitation sources were used. We used a HeNe laser (543 nm) from Meles Griot or a blue LED from Nichia Chemical Industries (Tokushima, Japan). When an LED was used, an excitation band-pass of 466 ± 26 nm[26] was selected using a 510-nm short-wave-pass filter. We also used an electroluminescent device, which was obtained from Lumitek International, Inc. (Ijamsville, MD). Its output was visually blue, with a maximum near 480 nm and a half-width of 80 nm. Polarizing plastic films were from Rolyn Optics (Covina, CA).

The fluorescence from RhB was observed through a 590-nm long-pass glass filter, and 6-CF was observed through a 540 nm wide band interference filter from Chroma Technology Corp.

Films of poly(vinyl alcohol) were prepared as described previously.[27,28] These films were physically stretched up to 6-fold to orient the MPSPI molecules, and the film was then pressed against the side of the cuvette (Chart 2). When stretched films are used, the stretching ratio (R_S) is defined as the axial ratio a/b of an ellipse formed when stretching an imaginary circle in

(16) Klimant, I.; Wolfbeis, O. S. Dual luminophore referenced optodes: A convenient way to convert the fluorescence intensity into a phase shift or time dependent parameter. *Europt(r)ode IV*; German Chemical Society: Berlin, 1998; pp 125−126.
(17) Neurauter, G.; Klimant, I.; Liebsch, G.; Kosch, U.; Wolfbeis, O. S. A comparative study on different types of intensity independent optical pCO_2 sensors. *Europt(r)ode IV*; German Chemical Society: Berlin, 1998; pp 231−232.
(18) Lakowicz, J. R.; Castellano, F. N.; Dattelbaum, J. D.; Tolosa, L.; Rao, G.; Gryczynski, I. *Anal. Chem.* **1998**, *70*, 5115−5121.
(19) Tolosa, L.; Gryczynski, I.; Eichhorn, L.; Dattelbaum, J. D.; Castellano, F. N.; Rao, G.; Lakowicz, J. R. *Anal. Biochem.* **1999**, *267*, 114−120.
(20) Lakowicz, J. R.; Dattelbaum, J. D.; Gryczynski, I. *Sens. Actuators*, submitted.
(21) Abugo, O.; Gryczynski, Z.; Lakowicz, J. R. *J. Biomed. Opt.*, submitted.
(22) Lakowicz, J. R.; Gryczynski, I.; Gryczynski, Z.; Dattelbaum, J. D. *Anal. Biochem.*, in press.
(23) Jabłoński, A. *Bull. Acad. Pol. Sci.* **1960**, *8*, 259−264.
(24) Weber, G. *Biochem. J.* **1952**, *51*, 145−155.
(25) Lakowicz, J. R. *Principles of Fluorescence Spectroscopy*, 2nd ed.; Plenum Publishers, Inc.: New York, Chapter 10, in press.
(26) Sipior, J.; Carter, G. M.; Lakowicz, J. R.; Rao, G. *Rev. Sci. Instrum.* **1996**, *67*, 3795−3798.
(27) Michl, J.; Thulstrup, E. W. *Spectroscopy With Polarized Light*; VCH Publishers: New York, 1986; p 573.
(28) Kawski, A.; Gryczynski, Z. *Z. Naturforsch.* **1987**, *42A*, 617−621.

Chart 2. Optical System for Anisotropy-Based Sensing with Visual Detection[a]

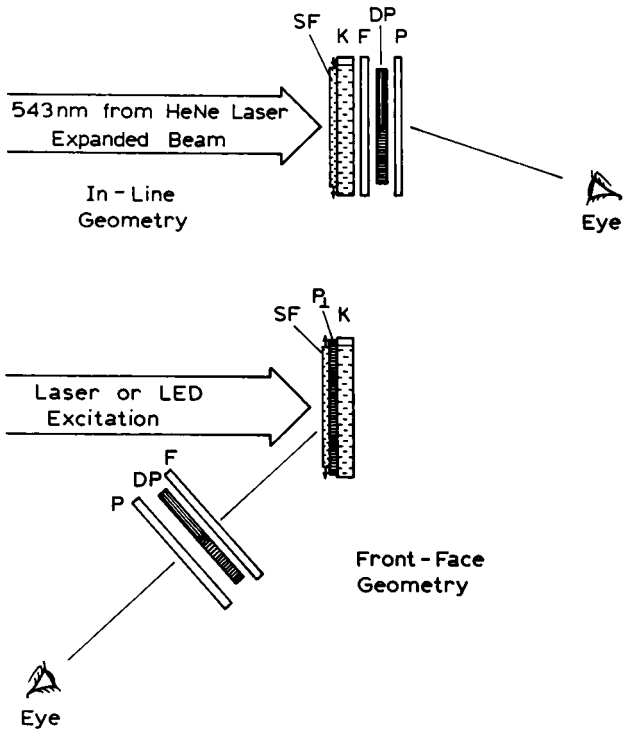

K – Cuvette

SF – Stretched PVA film doped with highly oriented dye; provides constant vertically polarized fluorescence background.

$P_{\perp}$ – Thin film polarizer oriented ortogonally to SF; transmits horizontal component of investigated fluorescence

F – Filter; transmits fluorescence, eliminates scattered excitation

DP – Dual Polarizer; plate combined with two "half moon" polarizers

P – Polarizer mounted in rotary stage

[a] (top) In-line geometry with the stretched film. (bottom) Front-face geometry. In the front-face geometry with the stretched film, it is possible to use an additional polarizer $P_{\perp}$ which allows selective detection of the horizontal component of the fluorescence from the sample cuvette K. Such a configuration extends the range of angles (angles needed to equalize the transmittance of both polarizers in DP) to 90°. Front-face anisotropy sensing can be performed without the additional polarizer, resulting in the 45° range of angles. It does not seem practical to use the polarizer $P_{\perp}$ in the in-line geometry when using an oriented film as the reference.

the unoriented film.[29] The volume of the circle or ellipse is assumed to be conserved. Under these conditions

$$R_s = N^{3/2} \tag{1}$$

where N is the physical fold of the stretch.

Stretched films provide an easily available reference fluorophore with a high polarization near unity. Such values can be obtained for fluorophores in stretched polymer films, which result in elongated fluorophores being aligned along the stretching axis.[27] In such systems, the electronic transitions of the fluorophore are all aligned in one direction or more precisely display a uniaxial orientation. The emission polarization from such samples are typically in the range of 0.6−0.8 and can approach 1.0.[28,29] Stretched polymer films retain their orientation for extended periods of time and thus can be practical for real-world applications.

THEORY

Operating Principle of the Visual Polarization Sensor. Schematic diagrams of two possible geometries for visual polarization sensing are shown in Chart 2. In the in-line geometry, the light passes through the sample. In the front-face geometry, the emission from the sample is viewed from the illuminated surface. In both cases, the absorption of the stretched film is adjusted so that the exciting light is only partially absorbed, and adequate intensity remains to excite the sample. A filter is used to eliminate the excitation and to transmit the emission.

An important part of the visual polarization sensor is the dual polarizer (DP). This component consists of two adjacent sheet polarizers with the optical axis of one rotated 90° relative to the other polarizer (Chart 2). If the sample is uniformly illuminated, the intensity transmitted by each half of the dual polarizer represents the parallel (||) and perpendicular (⊥) components of the emission. This emission has two components, from the reference film and from the sample.

Visual detection of the degree of polarization is accomplished by viewing the dual polarizer through an analyzer polarizer (P). This polarizer is rotated until the intensities are equal for both sides of the observation window. The total range of polarizer angles for the in-line geometry is 45°, as the emission ranges from 100% from the reference film to 100% from the sample. We found that it is easy to visually detect the position of equal intensities. As will be shown below, visual observation was found to provide 1° of accuracy in adjusting the analyzer polarizer.

The operating principle is the same whether the geometry is in-line or front face. However, the front-face geometry allows the use of an additional polarizer ($P_{\perp}$) after the stretched film but before the sample. This polarizer ($P_{\perp}$) can be used to selectively observe only the perpendicular component of the emission from the sample. As will be shown below, the use of $P_{\perp}$ increases the range of angles to 90°.

In-Line Geometry. In the biophysical use of fluorescence, it is common to use the anisotropy of the emission. However, in the present report, we are visually observing the emission from the front surface (front-face geometry) or directly through (in-line) the sample (in-line geometry). For these geometric conditions, we find it easier to describe the results in terms of the polarization of the emission,

$$P = (I^{\parallel} - I^{\perp})/(I^{\parallel} + I^{\perp}) \tag{2}$$

where $I^{\parallel}$ and $I^{\perp}$ are the intensities seen parallel (||) or perpendicular (⊥) to the orientation of the reference film.

The theory for visual detection of the polarization can be developed using Chart 3. This scheme shows the various polarized intensities from the sample (S) and reference (R) that are present

(29) Kawski, A.; Gryczynski, Z.; Gryczynski, I.; Lakowicz, J. R.; Piszczek, G. *Z. Naturforsch.* **1996**, *51A*, 1037−1041.

Chart 3. Polarizer Angles for In-Line Anisotropy Sensing[a]

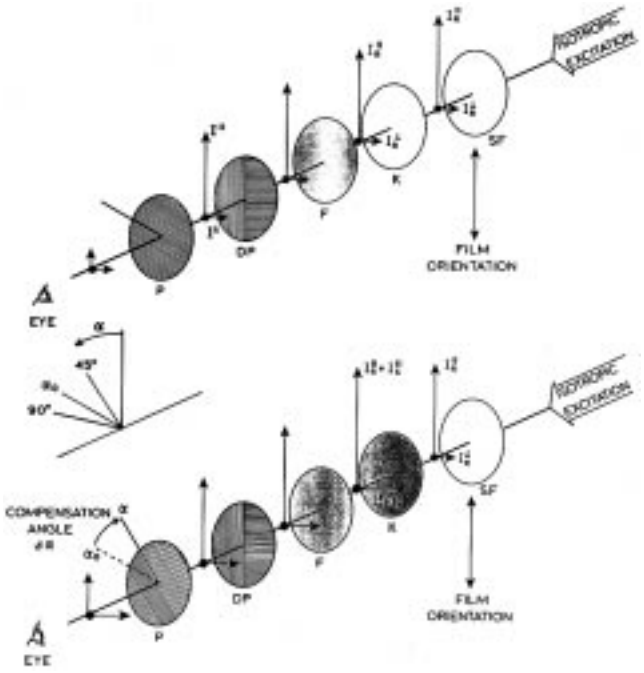

[a] In the top panel there is no emission from the sample. For a strongly oriented reference, the initial polarizer angle is near 90° from the vertical. In the lower panel, the sample emission is dominant, and the angle is near 45° from the vertical.

along the optical path. Suppose the sample is illuminated with unpolarized light. The emission from the stretched film is polarized along its stretch axis ($I_R^{\parallel}$). Since the alignment is never perfect, there is also a smaller component perpendicular to the stretch axis ($I_R^{\perp}$). The starting angle of the polarizer measured from the vertical axis (α_0) will be near 90°. The angle will be near 90° because the film emission is highly polarized, and the vertical component ($I_R^{\parallel}$) must be significantly attenuated to yield equal intensities in each half of the dual polarizer.

Suppose now there is significant emission from the sample (Chart 3, lower panel). Since the excitation is not polarized, and the sample is not oriented, the sample adds components of equal intensity in both directions ($I_S^{\parallel} = I_S^{\perp}$. We have assumed that the stretched film is optically thin, so that it does not act like a polarizer. The emission transmitted through each side of the dual polarizer is the sum of the two polarized components

$$I^{\parallel} = I_R^{\parallel} + I_S^{\parallel} \tag{3}$$

$$I^{\perp} = I_R^{\perp} + I_S^{\perp} \tag{4}$$

Assume now that these two components are observed through the analyzer polarizer. The intensities observed through the vertical (V) and horizontal (H) regions of the dual polarizer are given by

$$I^{V} = (I_R^{\parallel} + I_S^{\parallel}) \cos^2 \alpha \tag{5}$$

$$I^{H} = (I_R^{\perp} + I_S^{\perp}) \sin^2 \alpha \tag{6}$$

where α is the analyzer polarizer angle from the vertical position.

For visual measurement, the analyzer is rotated until the intensity is equal for both sides of the DP. For this condition one has

$$(I_R^{\parallel} + I_S^{\parallel}) \cos^2 \alpha = (I_R^{\perp} + I_S^{\perp}) \sin^2 \alpha \tag{7}$$

and

$$\tan^2 \alpha = (I_R^{\parallel} + I_S^{\parallel})/(I_R^{\perp} + I_S^{\perp}) \tag{8}$$

The stretched film displays a constant polarization value, which can be defined in terms of the ratio of the polarized intensities,

$$k = I_R^{\parallel}/I_R^{\perp} \tag{9}$$

For an isotropic film, there is no polarization and $k = 1$. Hence the initial angle for the analyzer polarizer is given by $\tan^2 \alpha_0 = 1.0$ or $\alpha_0 = 45°$. For a perfectly oriented film k equals infinity, $\tan^2 \alpha_0$ is very large so that α_0 is near 90°. In practice, one obtains highly but imperfectly oriented samples with values of k ranging from 10 to 12 in the case of isotropic excitation.

It is instructive to examine how the polarizer angle depends on the relative fluorescence intensity from the sample and the reference. Let the total intensity from the reference be defined as

$$I_R^{T} = I_R^{\parallel} + I_R^{\perp} \tag{10}$$

Dividing the numerator and denominator in eq 8 by I_R^T yields

$$\tan^2 \alpha = \frac{k/(k+1) + I_S^{\parallel}/I_R^{T}}{1/(k+1) + I_S^{\perp}/I_R^{T}} \tag{11}$$

For many situations the emission from the sample will be unpolarized, $I_S^{\parallel} = I_S^{\perp}$. For this condition one can define the ratio n, which is the ratio of the total emission from the sample to that of the reference,

$$n = I_S^{T}/I_R^{T} = (I_S^{\parallel} + I_S^{\perp})/I_R^{T} \tag{12}$$

Introduction of this ratio into eq 11 yields

$$\tan^2 \alpha = \frac{k/(k+1) + n/2}{1/(k+1) + n/2} \tag{13}$$

This expression (eq 13) describes the angle of the polarizer needed to equalize the intensities in terms of the polarization ratio of the reference (k) and the relative intensity of the sample to that of the reference (n).

It is informative to examine the range of polarizer angles that can occur as the intensity of the sample increases. The initial condition (α_0) is found when there is no emission from the sample, so that all the signal originates with the reference film. If the emission from the film were completely polarized ($k = \infty$), then the analyzer would need to be oriented at 90° to equalize the

intensities to zero. Basically, one would have to nearly extinguish the signal $I_R^{\parallel}$ by orienting the analyzer nearly perpendicular to the film axis.

In practice, the emission from the film is not completely polarized but is defined by a finite value of the *k* value. For a typical value of $k = 12$, the initial angle α_0 with no fluorescence from the sample is ~74°, which can be found using eq 13 with $n = 0$. Alternatively, one can calculate α_0 using

$$\tan \alpha_0 = \sqrt{k} \tag{14}$$

Now consider the condition when the emission from the sample is the dominant emission. We also assume that the sample emission is not polarized. Under these conditions the intensities I^V and I^H will be equal yielding $\tan^2 \alpha = 1.0$. The intensities seen through the analyzer will be equal when the analyzer is rotated 45° from the vertical. This value can be found by noting that as *n* becomes much larger than *k*, tan α approaches unity (eq 13) so α approaches 45°.

It is convenient to examine the changes in polarizer angle (Δα) in the absence and presence of sample. We call this value the "compensation angle". This change in angle is given by

$$\Delta\alpha = \alpha_0 - \alpha = \arctan \sqrt{k} - \arctan\sqrt{\frac{k/(k+1) + n/2}{1/(k+1) + n/2}} \tag{15}$$

Simulated values of Δα are shown in Figure 1 (top panel). These values were calculated for various values of *k*, and for a 10-fold range of relative intensities $n = I_S^T/I_R^T$. In the absence of fluorescence from the sample, the polarizer remains at the initial value near 90° with $\Delta\alpha = 0$. As the sample intensity increases, the polarizer must be rotated toward 45° to equalize the intensities. For experimentally accessible values of k near 12, the range of Δα values is ~30°. When the in-line geometry is used without the additional polarizer ($P_\perp$ in Chart 2), the range of angles depends on the orientation (*k*) of the film. The film must be oriented to some extent ($k > 1$) otherwise there is no change in the compensation angle. More highly oriented films, or larger values of *k*, yield larger changes in α.

Front-Face Geometry. The operational principles of the front-face polarization sensor (Chart 2, lower panel) can be understood by similar reasoning. The front-face sensor can be used without the extra polarizer $P_\perp$, in which case the range of angles is the same described above for the in-line geometry. An alternative approach is to use a polarizer $P_\perp$ in front of the sample. This polarizer selects for the perpendicular component of the sample emission. Under this condition, $I_S^{\parallel}$ is zero. Assuming the sample emission is unpolarized, the total emission from the sample is $I_S^T = I_S^{\perp}$, and eq 11 becomes

$$\tan^2 \alpha = \frac{k/(k+1)}{1/(k+1) + n} \tag{16}$$

The limiting conditions for the front-face sensor can be understood from Chart 4. In the absence of emission from the sample the, polarizer angle α_0 is defined by the value of *k*. For a perfectly aligned reference film ($k = \infty$) the analyzer polarizer must be oriented near 90° to equalize the intensities (top). At intermediate sample intensities (middle panel), the value of α to equalize the intensities will be between 0 and 90°. If emission from the sample is the dominant emission, then most of the emitted light is horizontally polarized, and the polarization angle must be near zero to equalize the signals (lower panel). This can be seen from eq 16. As *n* becomes large, tan α approaches zero, so α approaches zero. This result illustrates an important effect of using the additional polarizer $P_\perp$. The range of polarization angles doubles to 90° as compared to the in-line geometry without the polarizer $P_\perp$.

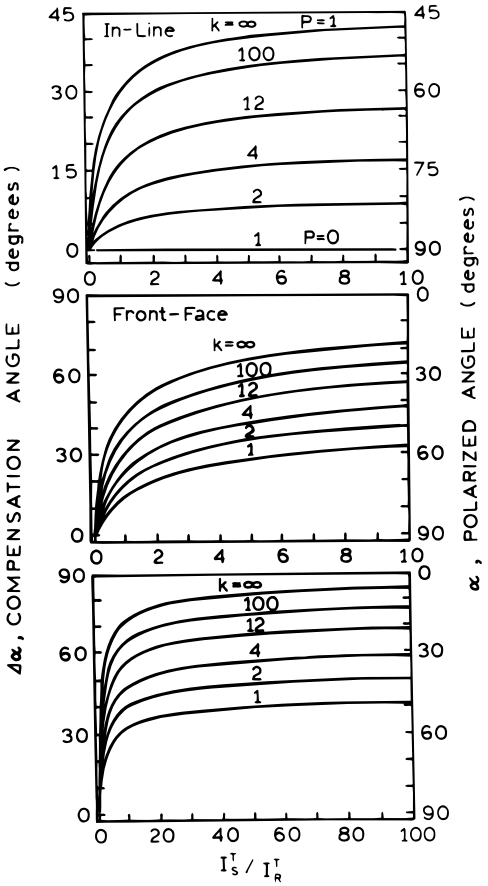

Figure 1. Calculated compensation angles for in-line anisotropy sensing (top) and front-face anisotropy sensing (middle and bottom). The lower two panels are similar, except for the scale of the *x* axis.

For the front-face sensor, the compensation angles Δα are given by

$$\Delta\alpha = \alpha_0 - \alpha = \arctan \sqrt{k} - \arctan\sqrt{\frac{k/(k+1)}{1/(k+1) + n}} \tag{17}$$

Simulated values of Δα are shown in Figure 1, middle and lower panels. As the sample intensity increases, the value of Δα approaches 90°. For available values of *k* near 12, Δα can be as large as 60°. Compared to the in-line geometry, it seems that a greater range of sample intensities can be measured using the front-face geometry than using the in-line geometry (lower panel).

The simulated values of Δα for the front-face geometry reveal another possibility, which is to perform anisotropy sensing without

Chart 4. Polarizer Angles for Front-Face Anisotropy Sensing[a]

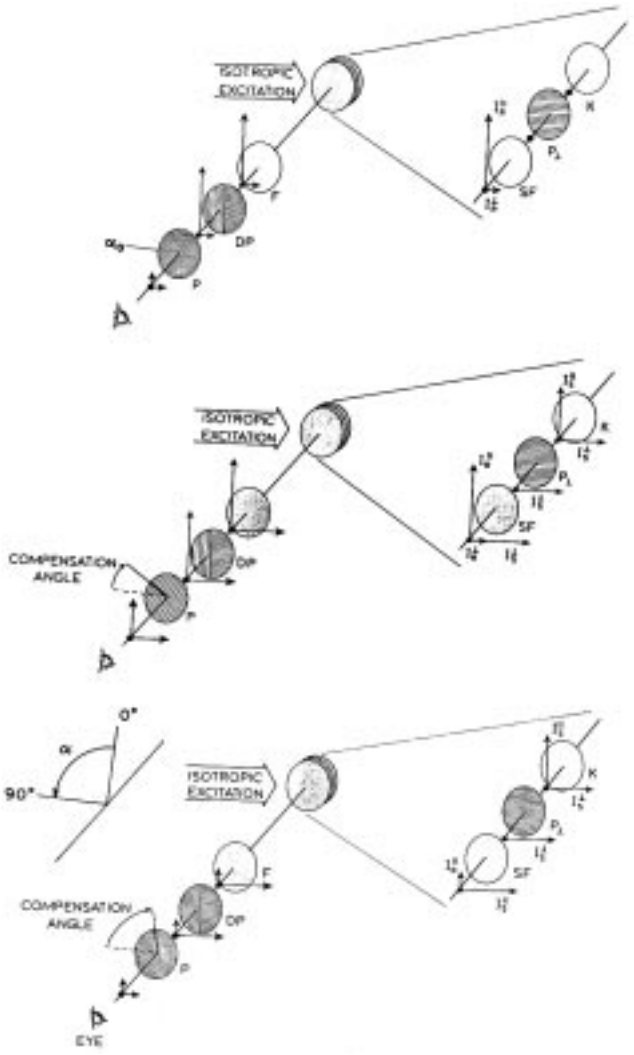

[a] In the top panel, there is no emission from the sample. For a strongly oriented reference film, the initial polarizer angle is near 90° from the vertical. In the bottom panel, the sample emission is dominant, and the angle approaches 0° from the vertical.

an oriented sample. This can be seen in Figure 1 (middle and lower panels) for $k = 1$, which is an unpolarized reference. A range of 45° is available using even an unpolarized reference. This possibility results from the additional polarizer $P_\perp$, which transmits only one polarized component from the sample. Since the reference can be unpolarized, the reference can consist of the sensing fluorophore itself, rather than a different fluorophore in an oriented film.

Precision of Polarization Sensing with Visual Detection. The principle of polarization sensing with visual detection is to equalize the light intensities transmitted through both sides of the dual polarizer. In our initial experiments, we were surprised to find that the polarizer angle could be determined to within 1°. As pointed out by the conscientious reviewer of this paper, the relative intensities change slowly for values of α near 45°, so that the precision we observed seemed to be unexpectedly high. For this reason we performed analyses to determine the expected precision of the α values.

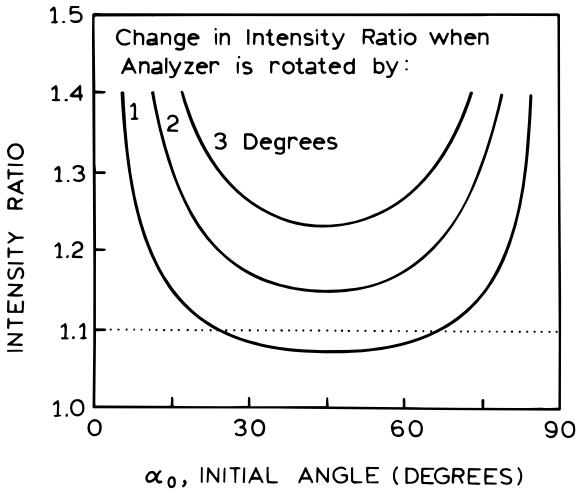

Figure 2. Dependence of the intensity ratio for change in α of 1, 2, or 3°. The *x* axis is the starting angle α_0. The intensity ratio was plotted as a value greater than unity.

The error in determining α should depend on the initial value of α (α_0), the accuracy of the rotary stage, and the sensitivity of our eyes to detect the intensity differences. Our rotary stage was accurate to 1°, and more accurate stages are readily available. Hence we considered the effects of various values of α_0 and the eye sensitivity. From eq 5 one can show that the relative intensity through each side of the dual polarizer is given by

$$I^{\mathrm{H}}/I_{\mathrm{V}} = \tan^2 \alpha \qquad (18)$$

We used this expression to calculate the relative change in intensity for changes in α of 1, 2, or 3° (Figure 2). If α_0 is close to 0 or 90°, the intensity ratio is strongly dependent on the polarizer angle α. For example, a change in α from 45 to 46° changes the intensity ratio to 1.072, and a change of 2°, 45 to 47°, results in a relative intensity change of 15%. Hence it appears that we must consider the sensitivity of the human eye to detecting relative intensities in adjacent images.

To answer the question of detectability of intensity differences we performed the following tests. We used a high concentration of RhB in ethanol to obtain a starting value near 45°. Next we inserted quartz plates in front of one side of the dual polarizer. The measured transmission of these plates were 93.4, 87.3, 81.8, and 76.1%, for one, two, three and four plates, respectively.

How many plates were needed to obtain a detectable intensity difference between the two sides of the dual polarizer? We were surprised that most of us could detect the presence of only one plate on either side of the dual polarizer. Everyone in this laboratory could recognize the presence of two plates, which provides an intensity difference of 1.14-fold or 14%. From these observations we judged that the average individual can detect an intensity ratio of 1.10, or a difference of 10%. This suggests that the polarizer angle can be adjusted to ~1.4° in the worst-case situation for α_0 near 45°.

We repeated these tests using a hand lamp and a red filter transmitting above 590 nm, with no sample or reference solution. Once again we could recognize a difference due to just a single plate. For angles from 0 to 25°, or from 65 to 90°, it is probable

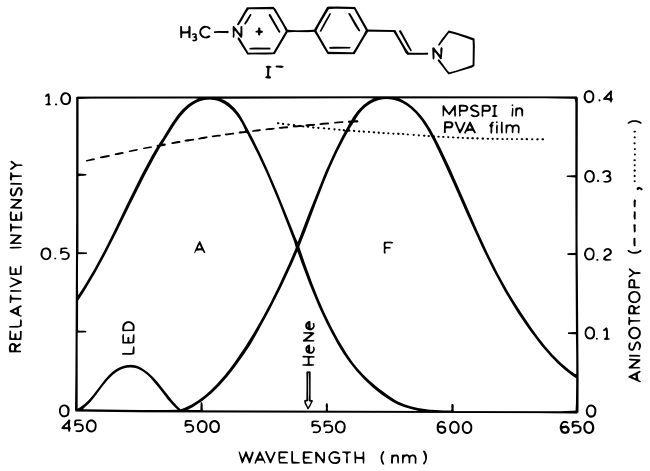

Figure 3. Absorption and emission spectra of the reference fluorophore MPSPI in an unoriented poly(vinyl alcohol) film. Also shown are the excitation and emission anisotropy spectra in the PVA film. The excitation wavelengths available from the LED and HeNe laser are indicated on the *x* axis.

that the accuracy of the polarizer angle can be greater than 1°. We did not perform such tests due to the limited resolution of our rotary stage. In summary, these results indicate that the accuracy in the polarizer angle should be 1° under most experimental conditions. This accuracy will be shown below to be adequate for typical sensing applications.

RESULTS

Polarization of an Oriented Film. Prior to showing examples of polarization sensing, it is valuable to discuss the spectral properties of the reference film. We chose the dye MPSPI because of its favorable absorption and emission spectra and its large Stokes' shift (Figure 3). MPSPI can be excited with either the 543-nm HeNe laser or the blue LED. Importantly, MPSPI displays a high fundamental anisotropy (r_0) across its absorption and emission spectra.

The elongated shape of MPSPI allows it to be strongly oriented in stretched poly(vinyl alcohol) (PVA) films. This is shown in Figure 4 which gives the fluorescence polarization as a function of the stretching ratio. As the stretching ratio increases, the polarization increases to over 0.8. It is valuable to notice that it is not necessary to use polarized excitation. The use of unpolarized excitation was mimicked by adjusting the excitation polarization at 45° from the vertical. Prior to stretching, the polarization is near zero for unpolarized (45°) excitation. However, for the stretched samples this polarization increases to over 0.8. The increase in polarization occurs irrespective of whether the film is excited with vertically polarized or unpolarized light. Hence, polarized emission from the reference film can be obtained without an excitation polarizer.

Polarization Sensing of RhB. To characterize the polarization sensor, we examined solutions of RhB in ethanol at various RhB concentrations. Initially we use the in-line geometry (Chart 2, top). Emission spectra are shown in Figure 5 for excitation at 543 nm. RhB displays a narrow emission with an emission maximum near 575 nm. The emission maximum of the MPSPI reference is at a similar wavelength, but the emission spectra of MPSPI is somewhat broader than RhB. As the RhB concentration increases,

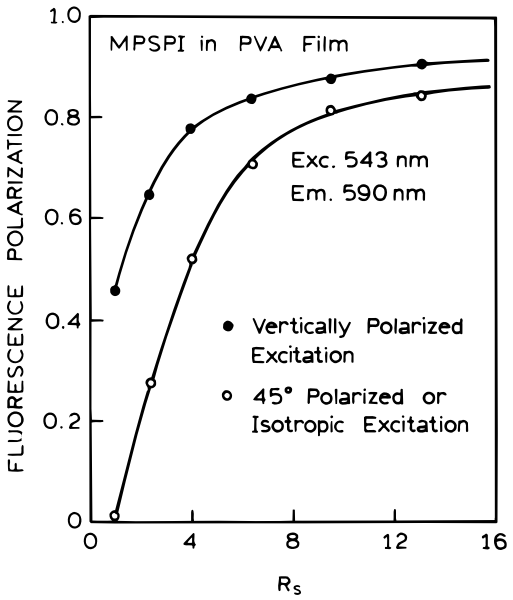

Figure 4. Fluorescence polarization of MPSPI in the PVA film as a function of the stretching ratio. The stretching ratio R_S is related to the actual physical fold of the stretch N by $R_S = N^{3/2}$ [29].

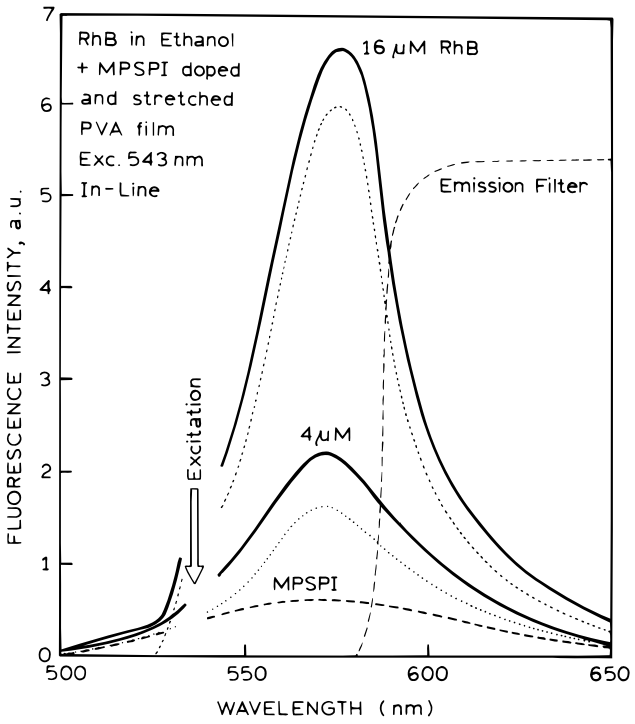

Figure 5. Emission spectra of rhodamine B in ethanol with (—) and without (···) with the MPSPI reference. The dashed line (- - -) shows the emission spectrum of MPSPI alone. The additional dotted line shows transmission profile of the emission filter.

its emission becomes dominant over that of the MPSPI reference. For the polarization measurements, the combined emission of MPSPI and RhB was observed using a filter that transmits above 580 nm.

Figure 6 shows the visual images seen through the analyzer polarizer for increasing concentrations of RhB. The polarization angle was initially adjusted to yield equal intensities in the absence of RhB. Since the reference film is highly polarized, the initial value α_0 is near 75°. All images were recorded with the analyzer

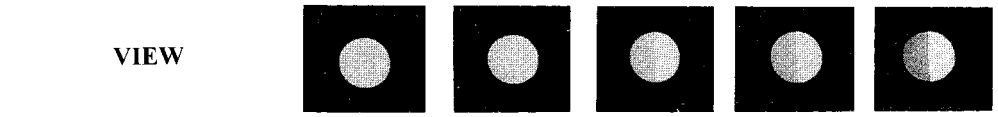

[Rhodamine B], μM	0	0.5	2	5	16
Compensation Angle (degrees)	0	3.5	10	14	22

Figure 6. Emitted light observed through the analyzer polarizer (P) for different concentrations of rhodamine B using the MPSPI reference and the in-line geometry. The position of the analyzer polarizer is at α_0 near 75° for all images. The listed values are the compensation angles ($\Delta\alpha$) needed to equalize the intensities.

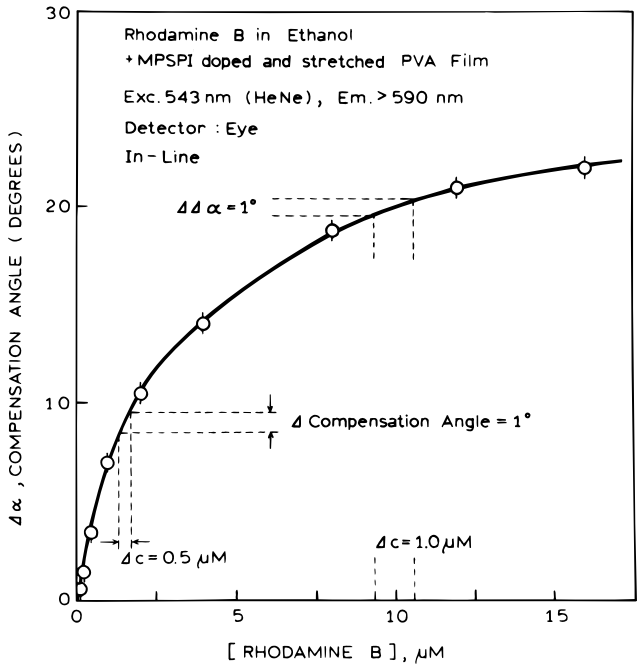

Figure 7. Dependence of the compensation angle ($\Delta\alpha$) on the concentration of rhodamine B using the in-line geometry (Chart 2, top). The uncertainty in the compensation angle is shown as $\Delta\Delta\alpha$.

polarizer in this same position. As the RhB concentration increases, the intensities through each side of the dual polarizer become unequal. The direction of the intensity changes can be understood by noting that the right side contains the horizontal polarizer and the emission from RhB is unpolarized. Addition of RhB results in an increased relative intensity on the right side, where the dual polarizer and the analyzer polarizer are in the horizontal position. The intensity increase is weaker on the left side, where the polarizers are nearly crossed.

Next we examined the changes in the polarizer angle, the compensation angle, needed to equalize the intensities seen from each half of the dual polarizer (Figure 7). To determine the compensation angle, we measured the difference between the analyzer angles needed to equalize the intensities in the absence and presence of the RhB sample. As the RhB concentration increased to 15 μM, the compensation angle increased by over 20°. During these measurements we asked several members of this laboratory to adjust the polarizer and measure the difference angle $\Delta\alpha$. Most individuals measured the same value of $\Delta\alpha$ to within 1°. It is interesting to consider the uncertainty in the RhB concentration resulting from the 1° uncertainty in the compensation angle. At low RhB concentrations, the uncertainty in 0.5 μM, or about one part in four. At higher RhB concentrations, the uncertainty is ~1 μM, or one part in ten. While this accuracy is somewhat poor, it is probably adequate for some clinical determinations, particularly those that report a yes/no answer rather than a specific value. We note that the range of concentrations is determined by the brightness of the reference film. Lower fluorophore concentrations could be measured if the reference film is less fluorescent.

Fluorophores in Scattering Media. In many situations it is desirable to measure the fluorescence from tissues, which can be due to intrinsic tissue fluorescence or due to extrinsic probes. Such measurements are becoming more important with the development of red or near-infrared (NIR) probes[30−32] and with the use of these probes for transdermal measurements.[33,34] Hence we decided to test the visual polarization sensor to measure the concentration of RhB in 0.5% intralipid. Such solutions are highly scattering and mimic the scattering properties of skin.

As for the previous case, RhB and MPSPI were excited at 543 nm using a HeNe laser. In this case we used the front-face geometry, as shown in Chart 2 (lower panel), including the polarizer ($P_\perp$) in front of the sample. The compensation angles are shown in Figure 8. Compared to the previous data for the in-line geometry (Figure 7), the front-face geometry results in a wider range of compensation angles, up to 30° or larger. This wider range is due to the additional polarizer ($P_\perp$), which selected only the horizontal component of the RhB emission. We did not notice any decrease in resolution due to the intralipid.

We note that it is not obvious that one can use polarization measurements to measure fluorophore concentrations in scattering media. It is well-known that light scattering results in depolarization of the emission from fluorophores within the scattering media. In the present situation this effect is not important because the polarization is imposed on the emission after it exits the scattering media.

Polarization Sensing of pH. As a practical illustration of polarization sensing, we used 6-CF as a pH-sensitive fluorophore.

(30) Daehne, S., Resch-Genger, U., Wolfbeis, O. S., Eds. *Near-Infrared Dyes for High Technology Applications, Proc. of the NATO Advanced Research Workshop on Syntheses*, Czech Republic, 1998; p 468.
(31) Thompson, R. B. Red and near-infrared fluorometry. In *Topics in Fluorescence Spectroscopy, Vol. 4: Probe Design and Chemical Sensing*; Lakowicz, J. R., Ed.; Plenum Press: New York, 1994; pp 151−181.
(32) Casay, G. A.; Shealy, D. B.; Patonay, G. Near-infrared fluorescence probes. In *Topics in Fluorescence Spectroscopy, Vol. 4: Probe Design and Chemical Sensing*; Lakowicz, J. R., Ed.; Plenum Press: New York, 1994; pp 183−222.
(33) Bambot, S. B.; Rao, G.; Romauld, M.; Carter, G. M.; Sipior, J.; Terpetschnig, E.; Lakowicz, J. R. *Biosens. Bioelectron.* **1995**, *10*, 643−652.
(34) Szmacinski, H.; Lakowicz, J. R. *Sens. Actuators B* **1996**, *30*, 207−215.

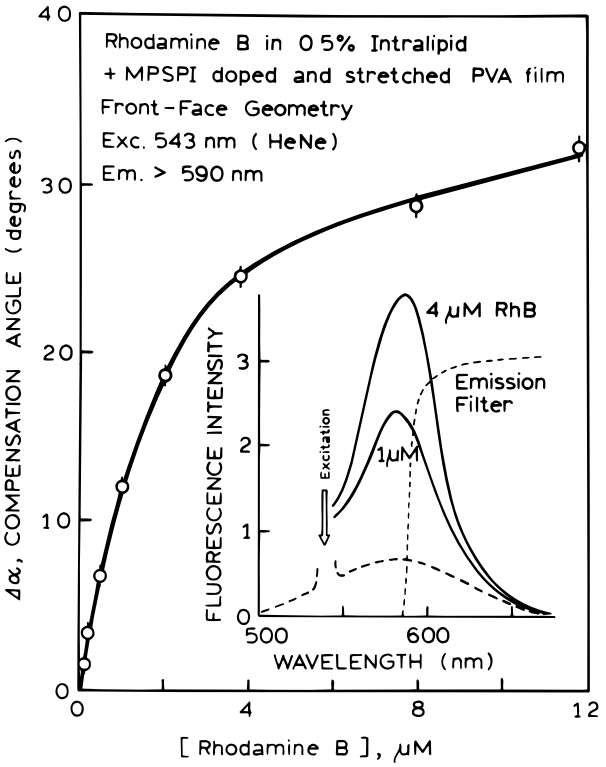

Figure 8. Dependence of the compensation angle on the rhodamine B concentration in 0.5% intralipid. These data were obtained using the front-face geometry (Chart 2, lower panel). The inset shows the emission spectra observed for the rhodamine B−MPSPI sample. The dashed line emission spectrum is of the MPSPI reference alone.

Fluorescein has been widely used as a pH-sensitive probe.[35−37] The pH-dependent fluorescence intensity is due to the carboxy group. Fluorescein is highly fluorescent at higher pH values where this group is ionized, and more weakly fluorescent at low pH. The intensity of fluorescein and its carboxy derivatives increases dramatically over the pH range from 5 to 8.

Figure 9 shows the emission spectrum of fluorescein in the front-face geometry, including the reference MPSPI film. In this case, excitation was accomplished with the 470-nm output of a blue light-emitting diode (LED). This solid-state light source can be powered by a 9-V battery. The fluorescein emission at 525 nm increases ~5-fold from pH 5 to 9. The emission of the MPSPI reference is at somewhat longer wavelengths. This illustrates one minor technical challenge in the design of a visual polarization sensor; the colors on each side of the dual polarizer can be slightly different due to the different relative intensities of the fluorophore and the reference. In the present case, we minimized these visual differences by selecting a relatively narrow range of wavelengths for visual observation, from 540 to 560 nm. In practice it should not be difficult to obtain similar visual colors for this sample and reference emission. A wide variety of fluorescent sensors are available,[8] and a large number of fluorophores can be oriented in stretched films.[27]

Compensation angles for the polarization pH sensor are shown in Figure 10. These angles display the usual sigmoidal behavior

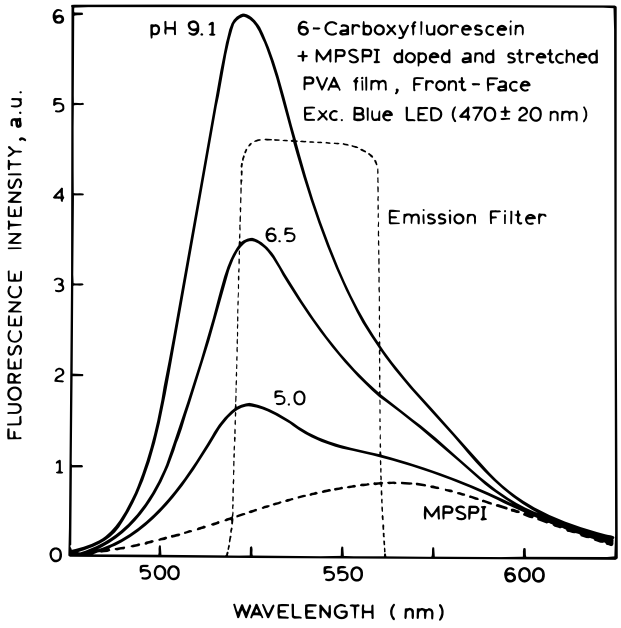

Figure 9. Emission spectra of a front-face anisotropy pH sensor based on 6-carboxyfluorescein. The dashed line shows the transmission profile of the emission filter used for the visual measurements.

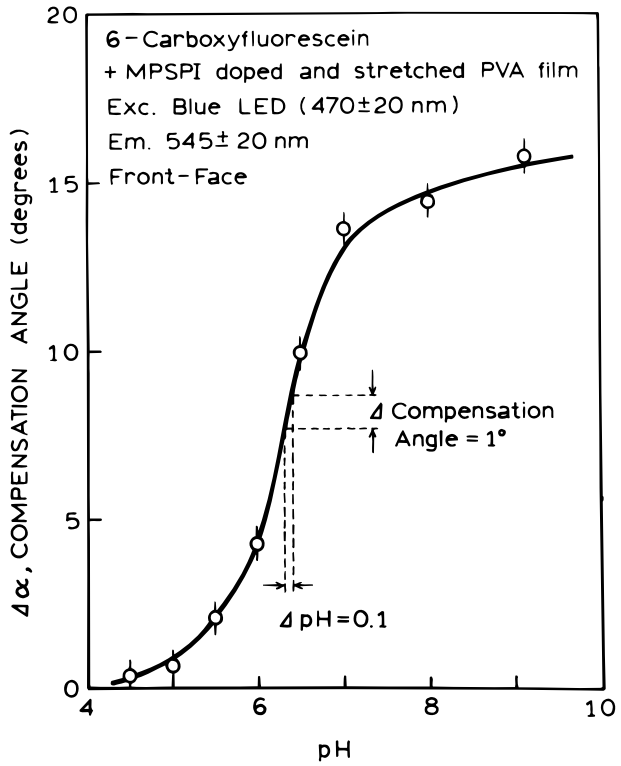

Figure 10. Compensation angles for the front-face polarization pH sensor.

for a pH sensor. For this initial visual pH sensor, the 1° accuracy of the compensation angle results in a pH accuracy to ±0.1 pH unit at the center of the titration curve. For clinical pH measurements, the required accuracy is ±0.02.[38−40] Hence, the present

(35) Babcock, D. F. *J. Biol. Chem.* **1983**, *258*, 6380−6389.
(36) Klonis, N.; Clayton, A. H. A.; Voss, E. W.; Sawyer, W. H. *Photochem. Photobiol.* **1998**, *67*, 500−510.
(37) *Molecular Probes Catalogue*, 6th ed.; Richard P. Haugland, Ed.; Molecular Probes, Inc.: Eugene, OR, 1996; pp 551−561.
(38) Mahutte, C. K.; Holody, M.; Maxwell, T. P.; Chen, P. A.; Sasse, S. A. *Am. J. Respir. Crit. Care Med.* **1994**, *149*, 852−859.
(39) Mahutte, C. K.; Sasse, S. A.; Chen, P. A.; Holody, M. *Am. J. Respir. Crit. Care Med.* **1994**, *150*, 865−869.

sensor is not adequate for use in blood gas measurements. However, an accuracy of ±0.1 pH unit is adequate in a wide range of less critical applications. We note that the pH accuracy is less than ±0.1 pH unit at pH values away from the central pH value near 6.5. This is a characteristic of any optical indicator based on a single dissociation constant.

It should be noted that the approach used for the fluorescein polarization sensor can be applied to a wide variety of analytes. The only requirement is a fluorophore that changes intensity in response to the analyte. Such fluorescent probes are known for a wide variety of species, including sodium, potassium, calcium, magnesium, zinc, chloride, phosphate, and oxygen.[41−50] Hence, visual sensors can be anticipated for a wide range of analytes.

Visual Polarization Sensing Using the Same Substance as the Reference. As a final illustration of polarization sensing, we show how the measurement can be accomplished using the same fluorophore as the sample and as the reference. This possibility was discussed above (Chart 2 and Figure 1) where we described the use of an additional polarizer in front of the sample to select the perpendicular component of the sample emission. The optical arrangement is shown in Figure 11 (top). In this case, the light source was an electroluminescent device which was powered by a 9-V battery. The output from the ELL was blue and centered near 480 nm.

To illustrate this method of visual sensing, we used a sample that contained varying concentrations of $[Ru(bpy)_3]^{2+}$. Such metal−ligand complexes are now being widely used as luminescent probes when covalently attached to macromolecules[51−55] and as chemical sensors.[56−61] As the reference, we used the same fluorophore $[Ru(bpy)_3]^{2+}$ at a constant concentration. The emission from this reference sample was viewed through a polarizer ($P_\perp$) to select just the perpendicular component at its emission. The combined emission from the sample and reference was then viewed through the dual-polarizer analyzer−polarizer combination. The optical arrangement is shown on the top of Figure 11.

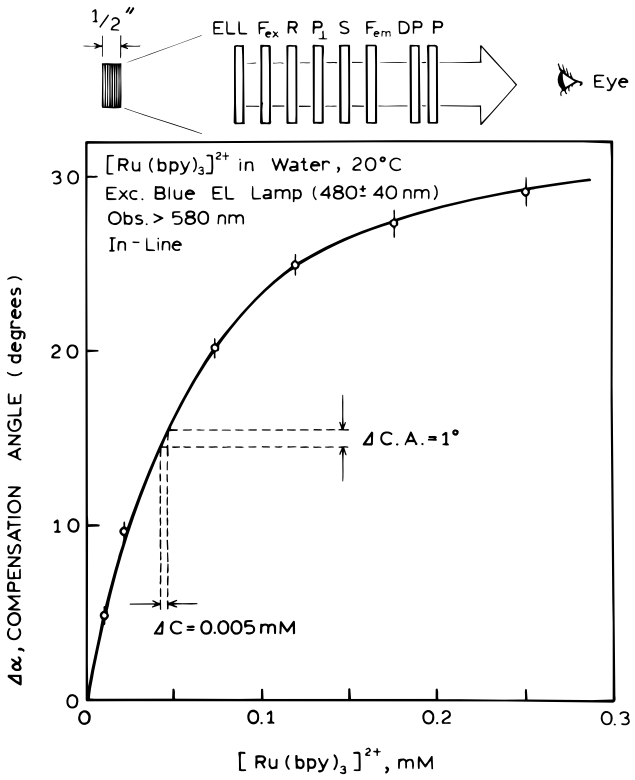

Figure 11. Visual detection of the concentration of $[Ru(bpy)_3]^{2+}$ measured using the same compound as the reference: ELL, electroluminescent light source; F_{ex}, excitation filter; R, reference solution with a constant concentration of $[Ru(bpy)_3]^{2+}$, $P_\perp$, polarizer; S, sample with varying concentrations of $[Ru(bpy)_3]^{2+}$, F_{em}, emission filter; DP, dual polarizer; P, analyzer polarizer.

The compensation angles for various concentrations of $[Ru(bpy)_3]^{2+}$ are shown in Figure 11. These angles are the differences between the polarizer angles needed to equalize the intensities in the absence and presence of the indicated $[Ru(bpy)_3]^{2+}$ concentration. These results demonstrated that visual polarization sensing is possible using the same fluorophore as the reference. This approach has the advantages of automatically providing the same visual wavelengths for the sample and reference and thereby avoiding any difference in color on each side of the dual polarizer.

It should be noted that these results suggest the use of visual polarization sensing in a number of common applications. Lumi-

(40) Mahutte, C. K. *Intens. Care Med.* **1994**, *20*, 85−86.
(41) Tsien, R. Y. Fluorescent indicators of ion concentrations. In Fluorescence Microscopy of Living Cells in Culture; Wang, L.-l., Taylor, D. L., Eds.; Methods in Cell Biology 29; Academic Press: New York, 1989; pp 127−156.
(42) Kao, J. P. Y. Practical aspects of measuring [Ca^{2+}] with fluorescent indicators. In A Practical Guide to the Study of Calcium in Living Cells; Nuccitelli, R., Ed.; Methods in Cell Biology 40; Academic Press: New York, 1994; pp 155−181.
(43) Lakowicz, J. R.; Szmacinski, H.; Johnson, M. L. *J. Fluoresc.* **1992**, *2*, 47−62.
(44) Lakowicz, J. R.; Szmacinski, H. *Sens. Actuators B* **1992**, *11*, 133−143.
(45) Kao, J. P. Y.; Harootunian, A. T.; Tsien, R. Y. *J. Biol. Chem.* **1989**, *264*, 8179−8184.
(46) Valeur, B. Principles of fluorescent probe design for ion recognition. In *Topics in Fluorescence Spectroscopy, Vol. 4: Probe Design and Chemical Sensing*; Lakowicz, J. R., Ed.; Plenum Press: New York, 1994; pp 21−48.
(47) Czarnik, A. W. Fluorescent chemosensors for cations, anions, and neutral analytes. In *Topics in Fluorescence Spectroscopy, Vol. 4: Probe Design and Chemical Sensing*; Lakowicz, J. R., Ed.; Plenum Press: New York, 1994; pp 49−70.
(48) Verkman, A. S.; Sellers, M. C.; Chao, A. C.; Leung, T.; Ketcham, R. *Anal. Biochem.* **1989**, *178*, 355−361.
(49) Biwersi, J.; Tulk, B.; Verkman, A. S. *Anal. Biochem.* **1994**, *219*, 139−143.
(50) Bacon, J. R.; Demas, J. N. *Anal. Chem.* **1987**, *59*, 2780−2785.
(51) Terpetschnig, E.; Szmacinski, H.; Lakowicz, J. R. Long-lifetime metal−ligand complexes as probes in biophysics and clinical chemistry. In *Methods and Enzymology*; Brand, L., Johnson, M. L., Eds.; Academic Press: New York, 1997; Vol. 278, pp 294−321.
(52) Szmacinski, H.; Terpetschnig, E.; Lakowicz, J. R. *Biophys. Chem.* **1996**, *62*, 109−120.
(53) Youn, H. J.; Terpetschnig, E.; Szmacinski, H.; Lakowicz, J. R. *Anal. Biochem.* **1995**, *232*, 24−30.
(54) Terpetschnig, E.; Szmacinski, H.; Lakowicz, J. R. *Anal. Biochem.* **1995**, *227*, 140−147.
(55) Guo, X.-Q.; Castellano, F. N.; Li, L.; Szmacinski, H.; Lakowicz, J. R.; Sipior, J. *Anal. Biochem.* **1997**, *254*, 179−186.
(56) Carraway, E. R.; Demas, J. N.; DeGraff, B. A. *Anal. Chem.* **1991**, *63*, 332−336.
(57) Demas, J. N.; DeGraff, B. A. *Anal. Chem.* **1991**, *63*, 829A−837A.
(58) Weidner, S.; Pikramenou, Z. *Chem. Commun.* **1998**, 1473−1474.
(59) Chang, Q.; Lakowicz, J. R.; Rao, G. *Analyst* **1997**, *122*, 173−177.
(60) Murtaza, Z.; Chang, Q.; Rao, G.; Lin, H.; Lakowicz, J. R. *Anal. Biochem.* **1997**, *247*, 216−222.
(61) Demas, J. N.; DeGraff, B. A. Design and applications of highly luminescent transition metal complexes. In *Topics in Fluorescence Spectroscopy, Vol. 4: Probe Design and Chemical Sensing*; Lakowicz, J. R., Ed.; Plenum Press: New York, 1994; pp 71−107.

nescent metal−ligand complexes have been used in immunoassays,[53,54] so that one can anticipate visual immunoassays based on intensity changes of metal−ligand complexes. Visual immunoassays may also be possible with the usual fluorophores with nanosecond decay times. Changes in the luminescence intensity can be caused by energy transfer or a variety of other mechanisms.[62,63] Another possible application is for industrial or household determination of oxygen, pH, or salt concentrations. Metal−ligand probes are known that are sensitive to oxygen[56,57] or pH,[60] and probes are known that are quenched by chloride.[48,49] Hence, one could develop visual sensors for these common analytes.

DISCUSSION

What are the advantages of polarization sensing with visual detection? One immediately obvious advantage is a simple device. The only electronic component is the light source. Excitation could be accomplished with LEDs, laser diodes, or electroluminescent devices. All this light sources can be powered using small batteries. Hence, one can readily imagine such sensors being developed for use in emergency health care, doctor's offices, and other medical applications. Additionally, the devices should be sufficiently inexpensive to allow their use in less critical situations such as bioprocessing and process control.

(62) Ozinskas, A. J.; Malak, H.; Joshi, J.; Szmacinski, H.; Britz, J.; Thompson, R. B.; Koen, P. A.; Lakowicz, J. R. *Anal. Biochem.* **1992**, *213*, 264−270.
(63) Hemmilä, I. A. *Applications of Fluorescence in Immunoassays*; John Wiley & Sons: New York, 1992; p 343.

It should be noted that the visual polarization sensor relies on intensity ratios and will thus be sensitive to any factor that alters the relative intensities of each polarized component. Hence the calibration curve will depend on the concentration and/or intensity of the sensing and reference fluorophores. If one fluorophore photobleaches at a rate different from the other fluorophore, then the calibration curve will change. However, we expect visual polarization sensors to be used with large-area low-intensity illumination, which should minimize photobleaching. Additionally, the inherent proximity focusing of the visual polarization sensor will avoid the intensity changes that occur with multiple optical components. Hence, we expect a visual polarization sensor to provide stable readings for extended periods of time.

In closing, we note that practical fluorescence sensing has been the goal of numerous research projects for the past 20 years. It now appears that the basic knowledge accumulated over these years can now be combined to yield simple and robust devices.

ACKNOWLEDGMENT

This work was supported by the NIH−National Center for Research Resources, Grant RR-08119.

Received for review November 23, 1998. Accepted January 13, 1999.

AC981301I